Optical design of liquid crystal lenses: off-axis modelling

Optical design of liquid crystal lenses: off-axis modelling

A.K. Kirby*, P.J.W. Hands, and G.D. Love
Durham University, Dept. of Physics, Durham, DH1 3LE UK.

ABSTRACT

We report on our work on producing liquid crystal switchable modal lenses and their use in a compound lens system in order to produce variable focus/zoom lenses. We describe work on producing a high power lens, and present theoretical work on off-axis phase modulation in a liquid crystal lens which is important in order to be able to carry out a complete optical design of a liquid crystal lens.

1. INTRODUCTION

Lenses with electronically controllable focal lengths for making variable focus/zoom lenses are currently producing considerable interest in both the technical and commercial literature. Technologies include electro-wetting[1,2], acousto-optics[3] and fluid-filled lenses[4]. Our work involves the use of modal liquid crystal (LC) lenses[5,6] in which a spatially varying voltage, and hence phase, is induced across a LC cell by using the equivalent electrical parameters of the cell. There are also many other methods of producing nematic LC lenses, many of which are reviewed in ref. 7. LC lenses have the advantage of being non-mechanical, robust, and requiring low operating voltages, but have the disadvantage of being of relatively low optical power. The natural question which arises is: can (modal) LC lenses be combined with other fixed conventional lenses to produce a compound lens with a useful range of variable focus/zoom. Despite the large numbers of papers published on liquid crystal lenses, there is very little published material on their optical design in complete systems. Wick *et al.*[8] published some preliminary results but they assume that the LC lenses act like conventional lenses.

In this paper we summarize the principle of modal LC lenses in the next section. We then go on to describe work on producing high power LC lenses. Next we describe work on calculating the phase shift in a LC cell as a function of the angle of incidence angle, which is important as a precursor for carrying out a complete optical design of an LC compound lens.

2. PRINCIPLE OF MODAL LC LENSES

A simple liquid crystal cell, composed of two conductive electrodes sandwiching the liquid crystal, is electrically equivalent to a capacitor with a small parasitic parallel conductance due to dielectric losses within the medium. If one of the electrodes is replaced with a material of higher resistivity and the dielectric losses ignored, then the equivalent circuit of the cell is as shown in figure 1(a) and can be modelled as a series of cascaded RC filters. If a sinusoidal voltage is applied to one end of the cell, the potential difference between the two electrodes therefore decreases as a function of distance across the device, as shown by the dotted lines in figure 1(b). The exact shape of the curve will depend upon the frequency and voltage of the applied potential, with higher frequencies generating more variation in voltage along the cell.

If both ends of the high resistance electrode are connected to the same driving voltage then the resultant potential across the device resembles a quasi-parabolic shape, as shown by the solid line in figure 1(b). The resulting phase profile across the device is an inversion of the voltage profile, due to the inverse relationship between voltage and retardance. The exact shape of the function is, in general, non-parabolic. However, careful control of the applied voltage and frequency can give a quasi-parabolic phase profile, similar to that required to generate a cylindrical lens. If we extend this idea further, into 2 dimensions, and connect the high resistance layer to the driving potential using an annular electrode, as shown in figure 2, then the result is a bowl-shaped electrical potential, and a phase profile that is similar to a spherical lens. Figure 3 shows the fringe patterns observed by placing excited LC lenses between crossed polarizers.

* a.k.kirby@durham.ac.uk

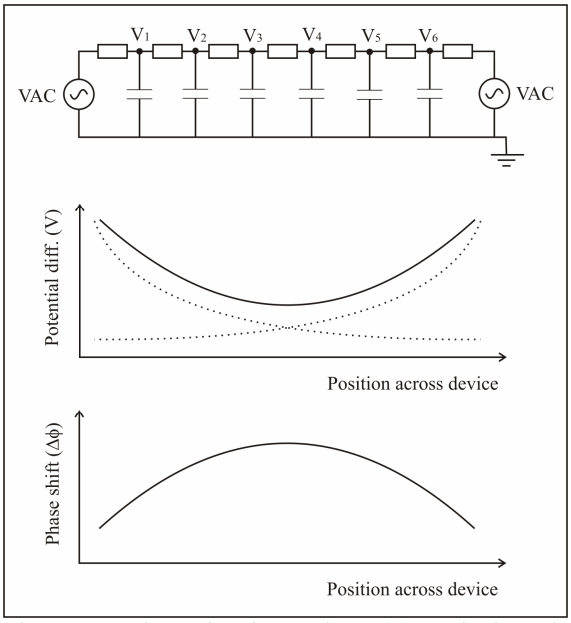

Figure 1. Schematic of a 1D lens: (a) Equivalent circuit of modal LC lens. (b) dotted line shows the voltage profile if a voltage is applied only to one end of a lens, and the solid lens shows the voltage profile if a voltage is applied to both ends.
(c) Resulting phase profile from a voltage being applied to both ends of a cell.

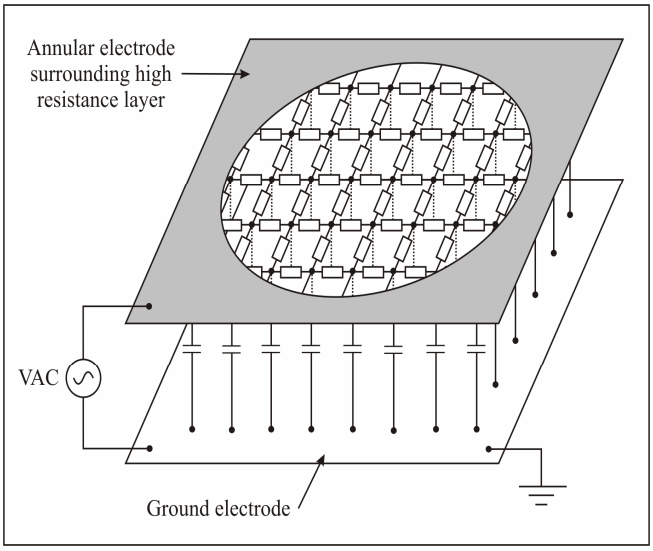

Schematic of a real 2D modal LC lens.

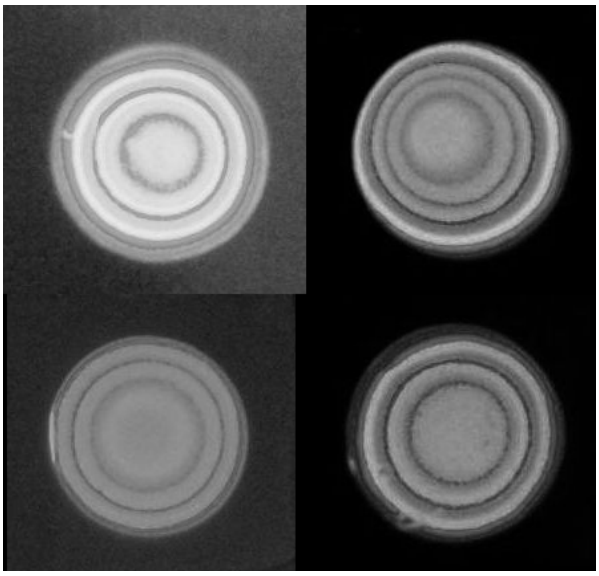

Figure 3. LC lens interference fringe patterns

3. HIGH POWER LC LENSES

The maximum achievable phase change produced by a nematic LC cell is given by $2\pi/\lambda \, \Delta n d$, where λ is the wavelength, Δn is the LC birefringence and d is the LC cell thickness. Apart from selecting a high birefringence material (materials with values of Δn up to 0.3 are available) the only way to produce a high stroke cell is to either increase the cell thickness or to make a device with multiple LC layers[9]. The latter has the advantage that there is then no prescribed maximum stroke, and the response time is not compromised by very thick cells. This is achieved at the expense of complexity. There is no clear data in the literature on the maximum cell thickness achievable. For very large values the LC alignment will be compromised since the molecules at the cell centre will be so far from the alignment layer.

We attempted building LC devices with an LC layer thickness of 100μm and 1mm. The LC material used was E7. The 100μm cell worked reasonably well, with good alignment and relatively little scattering. The maximum phase shift was measured to be 34.5(+/-0.25)λ (HeNe). Switching times were relatively slow, with a relaxation time-constant of approximately 24s. The 1mm cell showed poor alignment, and suffered from significant scattering. The degree of scattering could be reduced by applying a driving field, as expected, however no useful phase modulation was possible. By using a 100μm cell, with a 5mm lens diameter it should be possible to produce a lens with a minimum focal length of 7cm (f/14).

4. OFF-AXIS PHASE MODULATION IN A NEMATIC LC CELL

As a precursor to being able to produce optical designs of LC lenses it is important to calculate how the phase shift achievable in a LC lens varies as a function of off-axis angle. The vast majority of work on LCs is aimed at display applications, and there has been much work on maximizing the field of view of displays. However there is virtually no published work on how phase modulation varies as a function of angle.

The effect on the phase response of the off-axis angle depends on the azimuthal angle of incidence, and we therefore need to consider two situations. Firstly, when the incident plane of light (formed by the beam direction and the cell normal) is parallel to the LC directors, and secondly when the two are orthogonal. These two situations are described in the following two sub-sections. In both cases an ideal lens was assumed with the following specifications.

1. An ideal parabolic profile exists for normal incidence
2. Cell is exercised over its full dynamic range
3. Cell thickness of 50 μm
4. n_o=1.53, n_e=1.79
5. Lens diameter=10mm
6. Molecule angle is uniform throughout thickness of cell (no boundary effects).

The theoretical focal length for such a lens is 48cm. We then calculated the deviation from the ideal, as a function of off-axis angle. Therefore, the results give, by definition, zero aberration for an on-axis beam. In the first case (plane of incidence parallel to directors) the situation is relatively simple to model, and results of the phase aberrations are shown. The second scenario (plane of incidence orthogonal to directors) is more complicated – because polarization transformations are also involved. We therefore calculate the results using Jones calculus and express the results in terms of Strehl ratios.

4.1 Off axis behaviour in director plane.

An LC molecule can be modelled as an ellipsoid with a circular cross-section. The ordinary and extraordinary refractive indices correspond to the apparent length and width of the ellipsoid respectively, and vary with rotation under an external

field. The LC lens is aligned such that the polarization axis of the incident light is aligned with the extraordinary axis. For normal incidence, the effective refractive index of the LC material at a specific molecule angle, θ, is given by:

$$n_{eff} = \frac{n_o n_e}{\sqrt{(n_o \sin\theta)^2 + (n_e \cos\theta)^2}}. \quad (1)$$

n_{eff} is the effective refractive index, n_o is the ordinary refractive index of the LC material, n_e is the extraordinary refractive index of the LC material and θ is the LC molecule rotation angle, which is equal to 90^o in the off state.

Our model follows the following procedure

1. Calculate an ideal parabolic phase (and hence refractive index) profile using the specifications on the previous page in the introduction to this section.
2. By inverting equation 1. above, calculate how the LC director varies along the cell. We assume that the director is constant throughout the thickness of the cell and that there are no edge effects.
3. For a given off-axis angle, calculate a new effective LC director value, using the geometry shown in figure 4 below. From figure 4 it is clear that the modification to θ to give the effective molecule angle, ϕ, with an angle of incidence, δ, is simply the difference of angles $\phi=\theta-\delta$ (in the above figure θ and ϕ have opposite signs).
4. Calculate a new effective refractive index (for a given off axis angle), using equation 1 again.
5. Calculate a new effective cell thickness, d_{eff}, for off axis angles using $d_{eff} = \frac{d}{\cos\delta}$, where d is the cell thickness. We assume that refraction in the cell is negligible.
6. Calculation an off-axis phase function from a knowledge of the effective index profile (from 4 above) and the effective cell thickness (from 5 above).
7. Subtract the on- and off-axis phase profiles to calculate an aberration function.

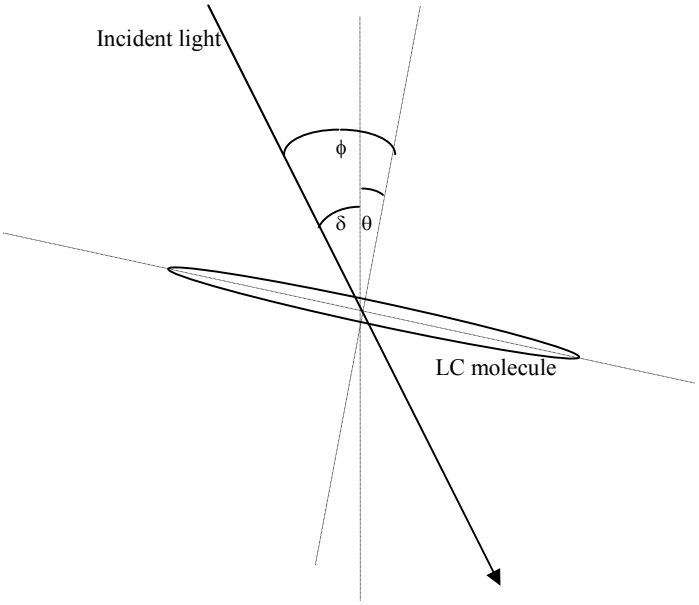

Figure 4. Off-axis incidence in the director plane. The ellipse represents a LC molecule. The vertical line is the cell normal, and the arrow shows the incident beam of light.

Figure 5 shows the resulting variation in the peak-valley (PV) aberration across the lens aperture with angle of incidence.

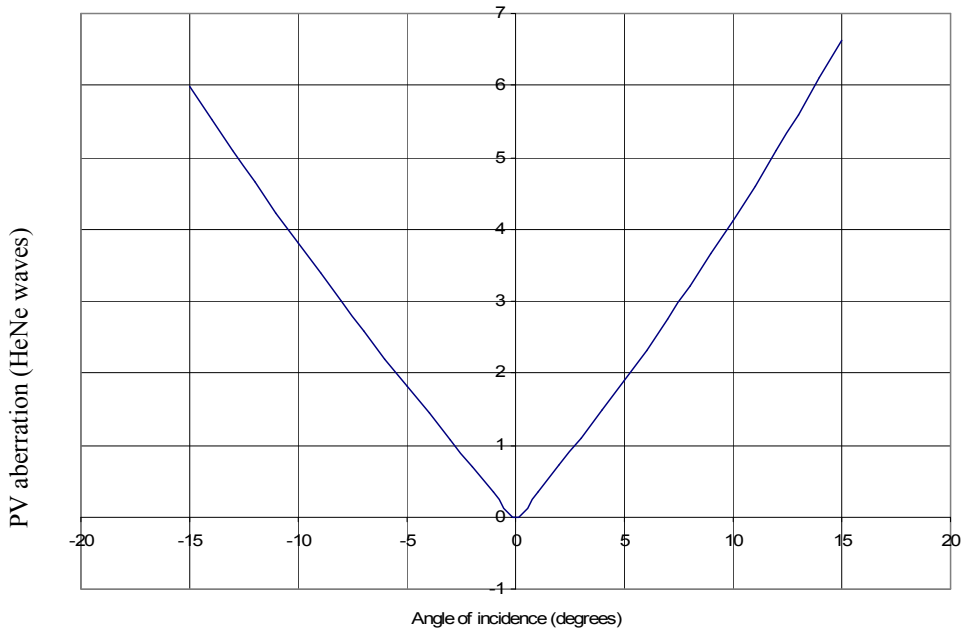

Figure 5. Calculated PV aberration vs. angle of incidence for a 48cm focal length LC lens when the plane of the off-axis light is parallel to the LC directors.

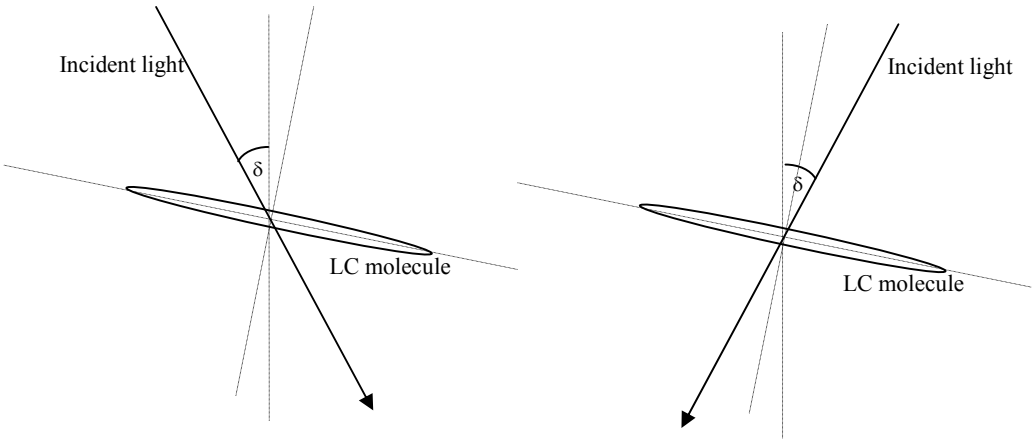

Figure 6. Comparison of positive and negative angles of incidence

It is apparent that there is an asymmetry between positive and negative angles of incidence, both in the aberration profiles and in the PV aberrations. This is to be expected from the geometry, as illustrated in figure 6. It is also apparent that the

aberrations are large for large off-axis angles. Although the modulus of the angle δ is equal in both cases, the effective angle with the LC molecule is obviously quite different. The asymmetry and the amount of aberration can be reduced by using a dual-layer cell with opposing LC molecule rotations, as shown in figure 7.

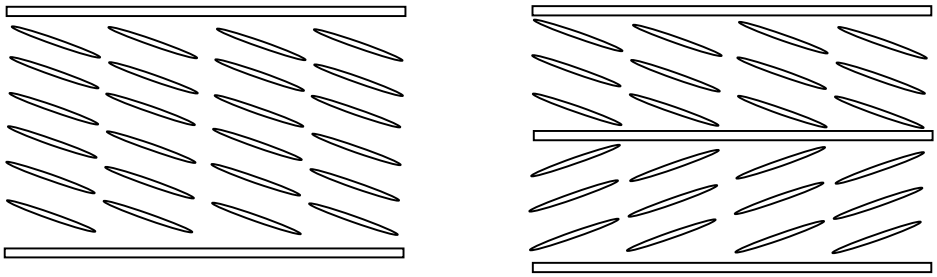

Figure 7. Single and Dual layer LC cells

The modelling of the dual layer lens is very similar to that of the single layer. The dual layer cell is treated as two individual single layer cells with opposite molecule angles, and the net optical path length is simply the sum of the optical path length of the two single layer cells. To normalise between the models, each layer in the dual layer cell was half the thickness of the single cell, giving the same overall thickness.

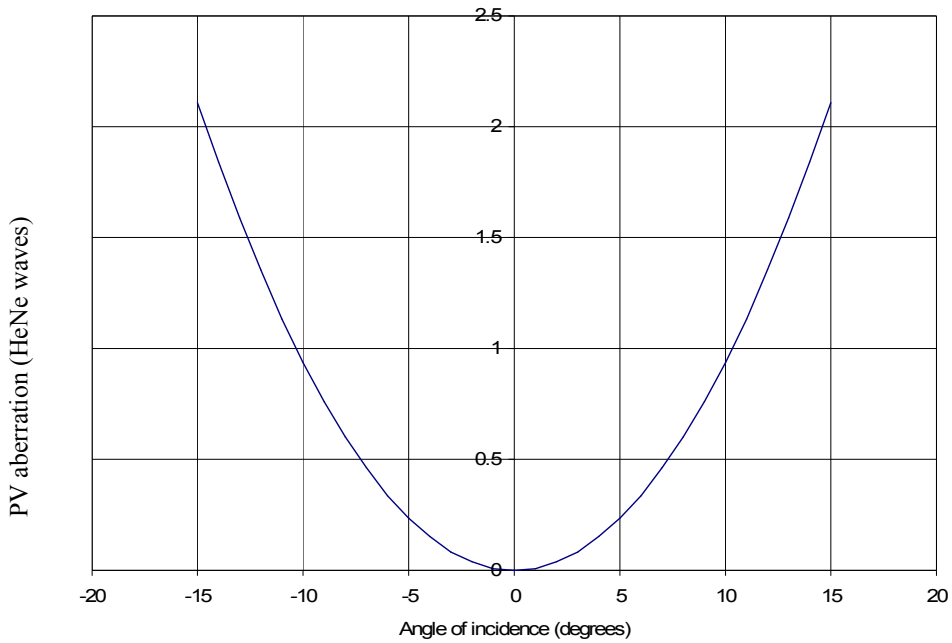

Figure 8 Calculated PV aberration vs. angle of incidence for a 48cm focal length dual LC lens (shown in fig 7) when the plane of the off-axis light is parallel to the LC directors.

From figure 8, it is clear that the asymmetry present in the single layer LC lens is not present in the dual layer cell. Furthermore, comparison of figures 5 and 8 shows that the aberrations are smaller for the dual layer lens, i.e. the off-axis performance of the dual layer lens is better than that of the single layer lens, despite identical on-axis performance.

4.2 Off axis behaviour orthogonal to director plane.

In the above case of off-axis incidence in the plane of the director rotation, the plane of polarization was always in the same plane as the LC director, and hence there were no polarization transformations. The situation is more complicated in the case of off-axis incidence orthogonal to the plane of director rotation, and the LC birefringence and resulting polarization transformations must be accounted for.

In this case our model is based on the following…

1. For a particular off-axis ray passing through the LC lens, the device appears to be a linear retarder with an apparent retardance, δ, at an apparent angle of ϕ.
2. To calculate δ and ϕ, as in the previous subsection, we first define an ideal refractive index profile for the on-axis case, and hence the required molecule angle profile.
3. Assuming incident linearly polarized light, calculate the emergent polarization state using Jones calculus and a knowledge of δ and ϕ.
4. The emergent state will, in general, be elliptical and it's precise state will vary across the cell. It is therefore not simple to produce simple aberration profiles as in the previous section. Instead we calculate resulting PSFs from the lens. By splitting the emerging elliptical states into horizontal and vertical components the result will be two (orthogonally polarized) components with varying phase and amplitude.
5. An aberration profile is calculated by subtracting the on- and off-axis phase profiles, and this is combined with the variation in amplitude to calculate, via a FFT, a resulting PSF.
6. There will be two PSFs, corresponding to each polarization state, and these are summed to calculate the final image.

This is now described in more detail below.

As the angle of incidence, ε, changes, the apparent orientation and refractive indices of the LC molecule change.

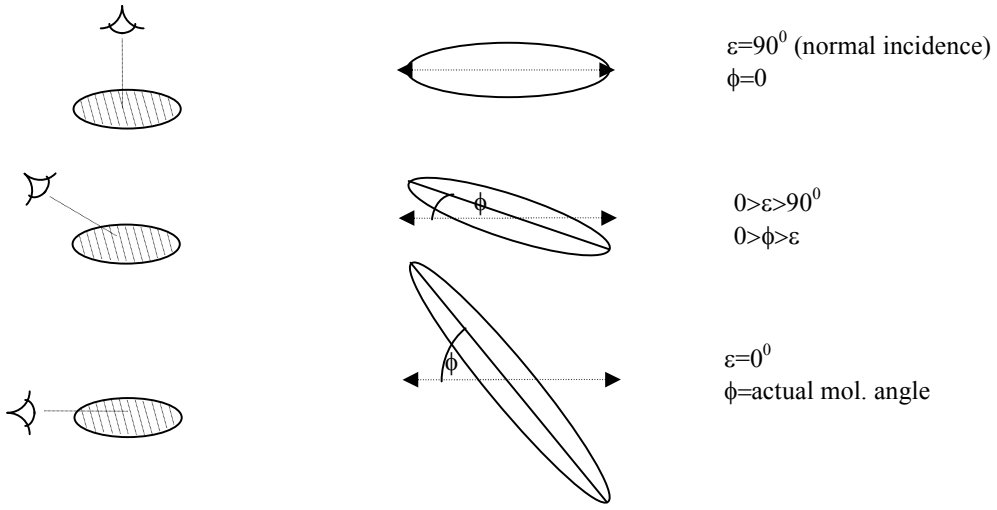

Fig. 9 Apparent molecule angle, ϕ, vs incidence angle, ε.

Figure 9 illustrates the variation in the apparent molecule angle with respect to angle of incidence. The dotted lines indicate the undeflected molecule alignment direction. The apparent molecule angle, ϕ, increases as the angle of incidence, ε, is varied, from $\phi=0$ at normal incidence (top) to a maximum of the actual molecule angle when $\varepsilon=0^0$.

The relationship between actual molecule angle (θ), apparent molecule angle (ϕ) and incidence angle (ε) is given by

$$\phi = \arctan\left(\tan(\theta)\cos(\varepsilon)\right) . \tag{7}$$

To calculate the phase term, δ, we need to calculate the effective refractive indices, n_{oeff} and n_{eeff}. Since the refractive index profile of the molecule is assumed to be a prolate spheroid, with long axis = n_e and short axes = n_o, the effective ordinary index, n_{oeff}, is always equal to n_o.

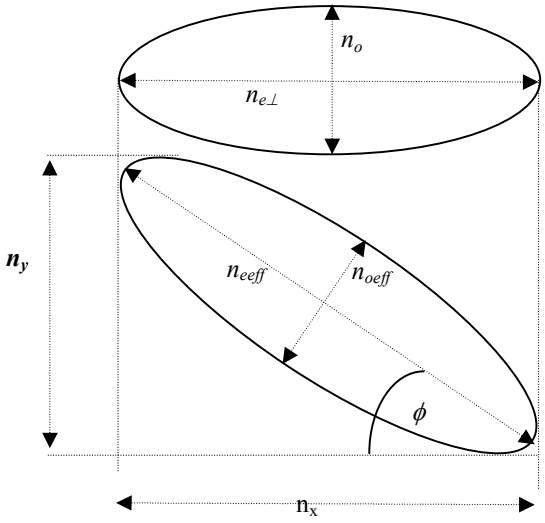

$n_x = n_{e\,eff}$ for normal incidence

Figure 10. Illustration of n_x, n_y

The quantity n_x is invariant with respect to angle of incidence, and is related to the apparent refractive indices of the molecule and the apparent molecule angle by equation 8.

$$n_x = \frac{n_o n_{eeff}}{\sqrt{{n_o}^2 \cos(\phi)^2 + {n_{eeff}}^2 \sin(\phi)^2}} . \tag{8}$$

Rearranging for n_{eeff} gives:

$$n_{eeff} = \frac{n_x n_o \cos(\phi)}{\sqrt{{n_o}^2 - {n_x}^2 \sin(\phi)^2}} . \tag{9}$$

In calculating the resultant retardance, δ, we must account for the change in the path length due to the incidence angle, ε. The retardance is given by:

$$\delta = \frac{(n_{eeff} - n_o)d}{\cos(\varepsilon)} \quad , \tag{10}$$

where d is the cell thickness. Jones calculus is used to calculate the properties of the emergent rays. The Jones matrix for a retarder of phase δ, at an angle ϕ is[13]:

$$R(\delta,\phi) = \begin{bmatrix} \cos(\phi)^2 e^{i\frac{\delta}{2}} + \sin(\phi)^2 e^{-i\frac{\delta}{2}} & \sin(\phi)\cos(\phi)e^{i\frac{\delta}{2}} - \sin(\phi)\cos(\phi)e^{-i\frac{\delta}{2}} \\ \sin(\phi)\cos(\phi)e^{i\frac{\delta}{2}} - \sin(\phi)\cos(\phi)e^{-i\frac{\delta}{2}} & \sin(\phi)^2 e^{i\frac{\delta}{2}} + \cos(\phi)^2 e^{-i\frac{\delta}{2}} \end{bmatrix} . \tag{11}$$

The normalised Jones vector is of the incident beam is given by:

$$J_i = \begin{bmatrix} 1 \\ 0 \end{bmatrix} \quad . \tag{12}$$

In the case of normal incidence, the emergent wavefront is, by definition, unaberrated, and so provides a useful reference for the general case. We use the Strehl ratio as our measure of the lens performance;

$$strehl = \frac{peak(psf_{Hor} + psf_{vert})}{peak(psf_{normal})} \tag{13}$$

For the simulation, a cell thickness of 50 μm, a diameter of 10mm, a focal length of 1m, a wavelength of 633 nm and LC refractive indices n_o=1.53, n_e=1.79 were used. Figure 3 shows the variation in Strehl ratio with off-axis angle = 0^0 to 10^0.

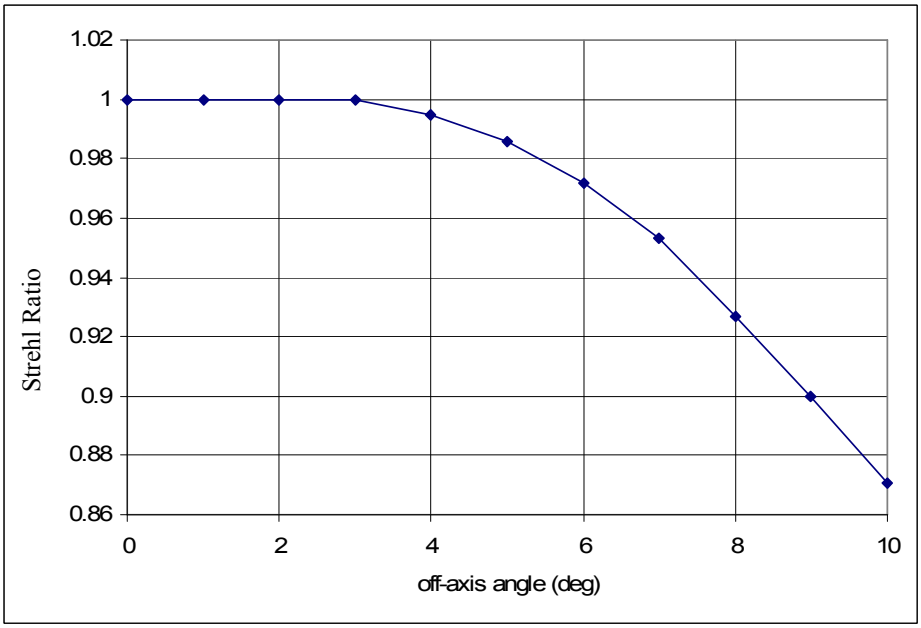

Figure 11. Strehl ratio vs off-axis angle

5. OPTICAL DESIGN OF LC LENS SYSTEMS

The analysis described in section 4 calculated the phase response and quantified the aberrations of an LC lens for two specific directions of off-axis incidence. A practical optical design requires a solution for the general case, which would ideally be incorporated into a professional optical design package, such as Zemax. In order to achieve this, a method of ray tracing in a spatially varying birefringent media is required. For convenience, the birefringence of a LC cell is normally considered to be a function of voltage. In reality, the birefringence of the LC material is fixed and it is the direction of the optical axes (the 'molecule angle' in the above analysis) which is a function of voltage - and which induces an *apparent* change in birefringence via a projection effect.
We therefore need to ray trace in a media where the direction of the optical axes are spatially varying. This complicates the modelling somewhat. Work has been carried out on this, and results of this work will be presented elsewhere.

ACKNOWLEDGEMENTS

This work was funded by the UK Particle Physics and Astronomy Research council. Thanks to our collaborators on this project – Richard Bingham, Mark Cropper, Steve Welch, and Andrew Griffiths (UCL, UK) and Charles Jenkins (Mount Stromolo Observatory, Australia). Thanks also for Alexander Naumov (Physical Optics Corp.) for his help and advice on LC lenses.

REFERENCES

1. S. Kuiper and H.H.W. Hendricks, `"Variable-focus liquid lens for miniature cameras"'. *Appl. Phys. Lett*. **85**(7):1128-1130 (2004)
2. Varioptic. http://www.varioptic.com
3. A. Kaplan, N. Friedman, and N. Davidson, "Acousto-optic lens with very fast scanning," *Opt. Lett*. **26**(14):1078-1080 (2001)
4. D.Y. Zhang, N. Justis, and Y.H. Lo. "Integrated fluidic adaptive zoom lens," *Opt. Lett*. **29**(24):2855-2857 (2004)
5. A.F. Naumov, M.Yu. Loktev, I.R. Guralnik, and G. Vdovin., "Liquid crystal adaptive lens with modal control," *Opt. Lett*. **19**(14):1013-1015 (1998)
6. A.F. Naumov, G.D. Love, M.Yu. Loktev and F.L. Vladimirov, "Control optimization of spherical modal liquid crystal lenses," *Optics Express* **4**(9):344-352 (1999).
7. L.G. Commander, S.E. Day, and D.R. Selviah,, "Variable focal length microlenses," *Optics Comms*. **177**:157-170 (2000)
8. D. Wick and T. Martinez, "Adaptive optical zoom," *Opt. Eng*. **43**(1): 8-9 2004
9. B.Wang, M.Ye, S.Sato, "Liquid crystal lens with stacked structure of liquid-crystal layers", *Optics Communications*. **250**:266-273 (2005)
10. H.W. Ren, Y.H. Fan, and S.T. Wu, "Polymer network liquid crystal for tunable microlens arrays," J. Phys. D: Appl. Phys. **37**, 400-403 (2004).
11. Y. Unno, "Point-spread function for a rotationally symmetric birefringent lens," *J. Opt. Soc. Am. A*. **19**(4):781-791 (2002)
12. S. Sanyal, Y. Kuwata, A. Ghosh, and S. Mandal, "Frequency response characteristics of a birefringent lens with off-axis aberrations." *Appl. Opt.* **43**(19):3838-3847 (2004)
13. W.Shurcliff, "Polarized light, Production and use", Harvard University Press, 1962